JCI The Journal of Clinical Investigation

# Soluble RARRES1 induces podocyte apoptosis to promote glomerular disease progression

Anqun Chen, … , Kyung Lee, John Cijiang He

*J Clin Invest.* 2020. https://doi.org/10.1172/JCI140155.

**Research** In-Press Preview **Cell biology** **Nephrology**

Utilizing the Nephrotic Syndrome Study Network Consortium and other publicly available transcriptomic datasets, we identified Retinoic acid receptor responder protein 1 (*RARRES1*) as a gene whose expression positively correlated with renal function decline in human glomerular disease. The glomerular expression of RARRES1, which is largely restricted to podocytes, increased in focal segmental glomerulosclerosis (FSGS) and diabetic kidney disease (DKD). Tumor necrosis factor-α (TNF-α) was a potent inducer of RARRES1 expression in cultured podocytes, and transcriptomic analysis showed the enrichment of cell death pathway genes with RARRES1 overexpression. The overexpression of RARRES1 indeed induced podocyte apoptosis in vitro. Notably, this effect was dependent on its cleavage in the extracellular domain, as the mutation of its cleavage site abolished the apoptotic effect. Mechanistically, the soluble RARRES1 is endocytosed and interacts with and inhibits RIO kinase 1 (RIOK1), resulting in p53 activation and podocyte apoptosis. In mice, podocyte-specific overexpression of RARRES1 resulted in marked glomerular injury and albuminuria, while the overexpression of RARRES1 cleavage mutant had no effect. Conversely, podocyte-specific knockdown of *Rarres1* in mice ameliorated glomerular injury in the setting of Adriamycin-induced nephropathy. Together, our study demonstrates an important role and the mechanism of RARRES1 in podocyte injury in glomerular disease.



**Soluble RARRES1 induces podocyte apoptosis to promote glomerular disease progression**

Anqun Chen[1,2]*, Ye Feng[2,3], Han Lai[2], Wenjun Ju[4], Zhengzhe Li[2], Yu Li[1], Andrew Wang[2], Quan Hong[2], Fang Zhong[2], Chengguo Wei[2], Jia Fu[2], Tianjun Guan[1], Bichen Liu[3], Matthias Kretzler[4], Kyung Lee[2]*, and John Cijiang He[2,5]*

[1] Division of Nephrology, Zhongshan Hospital, Xiamen University, Xiamen, China;

[2] Division of Nephrology, Department of Medicine, Icahn School of Medicine at Mount Sinai New York NY;

[3] Department of Nephrology, Institute of Nephrology, Zhong Da Hospital, Southeast University School of Medicine, Nanjing, Jiangsu, China;

[4] Division of Nephrology, Department of Internal Medicine, Department of Computational Medicine and Bioinformatics, University of Michigan, MI;

[5] Renal Section, James J. Peters VAMC, Bronx, NY

***Corresponding authors:**

John Cijiang He, MD/PhD, Kyung Lee, PhD, and Anqun Chen, MD.

Icahn School of Medicine at Mount Sinai
Department of Medicine, Division of Nephrology
One Gustave L. Levy Place, Box 1243
New York, NY 10029
Tel: 212 241 3568
Fax: 212 987 0389
Email: Cijiang.he@mssm.edu, kim.lee@mssm.edu, anqunchen@163.com

**Running title**: RARRES1 cleavage and its role in kidney cell injury

**ABSTRACT**

Utilizing the Nephrotic Syndrome Study Network Consortium and other publicly available transcriptomic datasets, we identified Retinoic acid receptor responder protein 1 (*RARRES1*) as a gene whose expression positively correlated with renal function decline in human glomerular disease. The glomerular expression of RARRES1, which is largely restricted to podocytes, increased in focal segmental glomerulosclerosis (FSGS) and diabetic kidney disease (DKD). Tumor necrosis factor-α (TNF-α) was a potent inducer of RARRES1 expression in cultured podocytes, and transcriptomic analysis showed the enrichment of cell death pathway genes with RARRES1 overexpression. The overexpression of RARRES1 indeed induced podocyte apoptosis in vitro. Notably, this effect was dependent on its cleavage in the extracellular domain, as the mutation of its cleavage site abolished the apoptotic effect. Mechanistically, the soluble RARRES1 is endocytosed and interacts with and inhibits RIO kinase 1 (RIOK1), resulting in p53 activation and podocyte apoptosis. In mice, podocyte-specific overexpression of RARRES1 resulted in marked glomerular injury and albuminuria, while the overexpression of RARRES1 cleavage mutant had no effect. Conversely, podocyte-specific knockdown of *Rarres1* in mice ameliorated glomerular injury in the setting of Adriamycin-induced nephropathy. Together, our study demonstrates an important role and the mechanism of RARRES1 in podocyte injury in glomerular disease.

Keywords: RARRES1, podocytes, apoptosis, DKD, focal segmental glomerulosclerosis (FSGS)

**INTRODUCTION:**

Podocytes are an integral component of glomerular filtration unit, and its injury leads to proteinuria and glomerulosclerosis in multiple glomerular diseases such as diabetic kidney disease (DKD) and focal segmental glomerulosclerosis (FSGS) (1). In DKD, the reduction in podocyte number or density correlates with the disease progression (2-4), and their detachment from the glomerular basement membrane and apoptosis upon injury are considered to be the two major mechanisms of podocyte loss in glomerular disease (5). As therapeutic options to prevent or reduce podocyte loss in glomerular disease are currently lacking, a better understanding of the mechanism of podocyte loss is warranted.

Retinoic acids (RA), the derivatives of vitamin A (retinol), are essential in control of epithelial cell growth and differentiation, as well as inhibition of inflammation (6). In addition to their established benefits in cancer chemoprevention (7), RA was shown to confer renoprotection in multiple experimental models of kidney disease (8, 9). However, these findings have not been translated into the clinical use for kidney disease, largely because of the lack of insight into the effects of RA in human kidneys in the setting of glomerular disease, and because RA can have significant toxicity in multiple tissues, particularly at high dosages (10, 11). Therefore, to better dissect the role of RA signaling in human glomerular disease, we utilized the transcriptomic datasets from patients with primary glomerular disease collected by Nephrotic Syndrome Study Network Consortium (NEPTUNE) and examined the expression of RA-related signaling molecules and target genes. The analysis showed that several of the RA-related genes indeed correlated with the progression of glomerular disease. Among these, the expression of retinoic acid receptor responder protein 1 (*RARRES1*, also known as Tazarotene-induced gene, *TIG1*) (12) was positively associated with the progression of primary glomerular disease, suggesting that *RARRES1* may be a risk gene for kidney disease. RARRES1, a type 1 transmembrane protein that was initially identified as a retinoic acid receptor-responsive gene (12), has since been reported to function as a tumor suppressor, as its expression is suppressed in various tumor cells (13) (14). However, the exact molecular mechanism of its anti-oncogenic effect is unclear, and the role of RARRES1 has not been explored in the context of kidney disease. Therefore, in this study we examined the role and mechanism of RARRES1 signaling in the pathogenesis of glomerular diseases.

**RESULTS:**

**Determination of RA-related signaling pathways and target gene expression in human glomerular transcriptomic datasets from NEPTUNE**

NEPTUNE is an NIH-funded consortium to study rare primary glomerular disease including minimal change disease (MCD), membranous nephropathy (MN), and focal segmental glomerular sclerosis

(FSGS) (15). Utilizing the collected NEPTUNE dataset of glomerular transcriptomic profiles from kidney biopsy samples of patients with primary glomerular disease, we examined the expression of a subset of RA-related signaling molecules and target genes that were identified in the previous studies with animal models (16, 17). Nearly 50% (26/52 genes) of RA-associated genes on the microarray chip were differentially regulated in the glomerular compartment in samples of at least one disease etiology in comparison with 6 healthy living donors. We further evaluated the correlation between gene expression levels with clinical parameters of kidney function, estimated glomerular filtration rate (eGFR) and protein-to-creatinine ratio (PCR), and disease progression rate, as quantified using eGFR slope by a mixed-effects model (**Table S1**). Among these, *RARRES1* expression correlated with eGFR slope (**Table S1**), as well as with renal function as assessed by eGFR, serum creatinine, and blood urea nitrogen (BUN) levels (**Figure 1A, Figure S1**). Since the correlation of *RARRES1* with eGFR slope suggested that RARRES1 might be associated with kidney longitudinal outcome, we evaluated the association between *RARRES1* expression and composite endpoint (end-stage renal disease or a 40% reduction of baseline renal function using the Cox regression model). During an average follow-up time of 25.6 months (range: 1 to 50 months), 28 out of 190 patients progressed to composite endpoint. Higher expression of RARRES1 was significantly associated with increased risk of progression to ESRD or a 40% reduction of baseline eGFR (**Figure 1B**), suggesting that RARRES1 is a risk gene associated with the progression of primary glomerular disease.

**Expression and localization of RARRES1 in the normal and diseased kidney**

To further validate the potential role of RARRES1 in kidney disease, we further queried the published transcriptomic datasets in kidney disease compiled in the Nephroseq database (*nephroseq.org*). *RARRES1* mRNA expression was significantly increased in the glomeruli of DKD patients compared with healthy controls (18), and its expression significantly correlated with eGFR in both CKD and DKD patients (**Figure S2**). Notably, recent single-cell RNA sequencing datasets of mouse kidney or glomeruli (19, 20) indicated that *Rarres1* is expressed predominantly in podocytes (**Figure S3A-B**) (19, 20) (19, 20). Our recent single-cell transcriptomic data of glomerular cells from diabetic mouse kidneys (21) confirmed that the expression of *Rarres1* was largely restricted to podocytes in both the normal and diabetic kidneys (**Figure S3C**)(21). Immunohistochemical staining showed low abundance of RARRES1 in the kidney biopsy samples of patients with minimal change disease, but significantly increased expression in the glomerular cells of the kidney biopsies from patients with DKD and FSGS (**Figure 2A-B**; clinical patient characteristics are listed in **Table S2**). Immunofluorescence staining showed that RARRES1 expression largely co-localized with the podocyte marker, Podocin, and further increased in DKD patients (**Figure 2C**).

**RARRES1 expression is induced by TNF-α in cultured human podocytes**

Since RARRES1 expression is mostly in podocytes and increased in the diseased kidney, we next examined how RARRES1 expression is upregulated using the conditionally immortalized human podocytes. We first confirmed that RA induced RARRES1 expression in a dose-dependent manner (**Figure S4A**). Interestingly, we found that TNF-α was more potent in the induction of RARRES1 than RA in human podocytes (**Figure S4B-C**), suggesting that in the kidney disease settings such as DKD and FSGS, RARRES1 expression is likely upregulated by TNF-α.

**RARRES1 is cleaved and secreted extracellularly**

RARRES1, as a type 1 membrane protein, is composed of a short N-terminal intracellular region, a single membrane-spanning hydrophobic region, and a large C-terminal extracellular region containing a glycosylation signal (**Figure S5A**). Cellular fractionation confirmed the membrane localization of RARRES1 in transfected podocytes expressing the V5-tagged RARRES1 (RARRES1-V5) (**Figure 3A**). Interestingly, a large extent of RARRES1 expression was found in the supernatant in RARRES1-V5 overexpressing podocytes (**Figure 3B**), suggesting that RARRES1 is cleaved and released extracellularly. The presence of cleaved RARRES1-V5 was confirmed by mass spectrometric analysis of supernatant proteins (data not shown). To further verify the cleavage on the extracellular domain of RARRES1, we overexpressed RARRES1 with either a C-terminal V5 tag or RARRES1 with a N-terminal FLAG tag, which would remain tethered to the plasma membrane (**Figure S5A-C**). As anticipated, while C-terminal V5 tagged RARRES1 was detected in the supernatant with both anti-V5 and anti-RARRES1 antibodies (**Figure 3B**), RARRES1 was detectable only by anti-RARRES1 antibody, but not by anti-FLAG antibody in the supernatant (**Figure 3C**), further confirming that the C-terminal portion of RARRES1 is cleaved and released extracellularly. The cleaved RARRES1 in the supernatant migrated as a larger protein than RARRES1 in the cell lysate (**Figure 3B**), suggesting that it may be highly glycosylated. Indeed, the de-glycosylation treatment of the supernatant proteins resulted in faster migration of the protein, similar to the size of the form found in the cell lysate (**Figure 3D**).

We next interrogated the potential cleavage site of RARRES1 by site-directed mutagenesis. We hypothesized that the cleavage may occur proximal to the transmembrane region near amino acids (aa) 21-42 (**Figure S5D**) and constructed two deletion mutants of RARRES1 with a C-terminal V5-tag: RARRES1 with a larger deletion segment of amino acids (aa) 43-76 (△aa43-76-V5) and RARRES1 with a smaller deletion of aa43-55 (△aa43-55-V5). The analysis of RARRES1 in the supernatant fraction in comparison to the cell lysate showed that while △aa43-55-V5 was able to be cleaved, △aa43-76-V5 could not, indicating that the cleavage site may be located between aa56-76.

*In silico* analysis to predict cleavage site by enzymes from metalloproteinase (MMP) family (www. cleavpredict. sanfordburnham.org; www.uniprot.org; http://web.expsay.org/peptide mass/)

suggested that aa68-71, encoding FFNF, may be the potential MMP cleavage site. Therefore, we constructed the mutant plasmid with the deletion of aa68-71 (△FFNF-V5), or substitution of FFNF with AAAA (AAAA-V5). Both mutations abolished the cleavage of RARRES1 (**Figure 3F**), confirming that aa68-71 are essential for the cleavage of RARRES1. We further made point mutations of aa68-71 (encoding FFNF) as follows: AFNF, FANF, FFAF, FFNA, and FFDF (underlined aa changed to A or D in FFNF). The substitution of aa70 (N) by either A or D (FFAF and FFDF) abolished the cleavage of RARRES1, while substitution by AFNF and FANA did not affect the cleavage, indicating that aa70 is essential for the cleavage. (**Figure 3F**). Indeed, the cleavage of RARRES1-V5 was mitigated when cells were treated with broad spectrum MMP inhibitor, Marimastat (**Figure 3G**). Moreover, the cleaved RARRES1 in the supernatant fraction was not largely derived from ectosomes, since isolated ectosomes from transfected cells contained a minimal amount of wildtype or cleavage mutant RARRES1 (**Figure 3H**).

**Podocyte apoptosis caused by the overexpression of RARRES1 is mitigated by the mutation of its cleavage site**

To examine the role of RARRES1 in podocytes, we next performed RNA sequencing of immortalized human podocytes with overexpression of RARRES1-V5. The pathway analysis indicated that top pathways with differentially expressed genes (DEGs) were in pathways of cell migration and apoptosis (**Table S3**). We also performed RNA sequencing of podocytes with *RARRES1* knockdown and stimulated with or without TNFα. The top DEGs stimulated by TNFα but suppressed by *RARRES1* knockdown, were enriched in cell cycle-related pathways (**Table S4**). Together, these analyses suggested that RARRES1 plays a key role in the regulation of cell cycle and apoptosis, consistent with its purported role as a tumor suppressor. Indeed, we found that the overexpression of wildtype RARRES1 (RARRES1-V5) in podocytes induced apoptosis as demonstrated by Annexin V-staining and western blot analysis of cleaved Caspase 3 levels (**Figure 4A-B**). Importantly, the overexpression of cleavage mutant RARRES1 (FFAF-V5) did not induce apoptosis in transfected podocytes, indicating that the cleavage of RARRES1 is required for the pro-apoptotic effects of RARRES1 (**Figure 4A-B**). The incubation of podocytes with 10ng/mL of soluble RARRES1 (sRARRES1-V5) isolated from supernatant collected from RARRES1-V5-overexpressing HEK293T cells induced apoptosis (**Figure 4C-D**). Interestingly, V5-tagged soluble RARRES1 in the supernatant of cultured HEK293T cells overexpressing RARRES1-V5 were also found in the cell lysates of the podocytes post-treatment (**Figure 4D**), suggesting that the soluble RARRES1 was taken up by podocytes. To determine whether this uptake was occurring through the endocytic process, we pretreated cells with a dynamin inhibitor (Dynasore) to block endocytosis. Indeed, endocytosis inhibition blocked the uptake of exogenous soluble RARRES1 in cultured podocytes (**Figure 4E**), and

blocked the podocyte apoptosis induced by soluble RARRES1 (**Figure 4F**). Together, these results indicate that podocyte apoptosis is a consequence of the endocytic uptake of cleaved RARRES1 that subsequently triggers an intracellular signaling cascade to activate the pro-apoptotic pathway.

**RARRES1 interacts with RIOK1 to induce apoptosis of podocytes**

To explore which membrane proteins or intracellular signaling molecules interact with RARRES1 to activate the apoptosis, we performed the immunoprecipitation/mass spectrometry analysis using cell lysates from podocytes overexpressing RARRES1-V5 or control vector. The immunoprecipitated proteins were largely intracellular proteins (**Table 1,** top 10 proteins are shown). Interestingly, RIOK1, an atypical protein kinase known to be involved in cell survival (22), was ranked top 4 on the list (**Table 1**). We further confirmed the interaction between RARRES1-V5 and myc-DDK-tagged RIOK1 (RIOK1-myc-DDK) by co-immunoprecipitation and western blotting. While the wildtype RARRES1-V5 interacted with RIOK1, the cleavage mutant FFAF-V5 could not (**Figure 5A**), suggesting that the cleavage of RARRES1 into soluble form is required for this interaction. As RIOK1 is an intracellular protein kinase, it is likely that cleaved RARRES1 that is endocytosed subsequently interacts with RIOK1. Consistent with the known function of RIOK1 to mediate the anti-apoptotic effect by inhibition of p53 activation (22), the overexpression of RIOK1 in podocytes abolished the effect of RARRES1 on p53 phosphorylation and cleavage of caspase 3 (**Figure 5B**), suggesting that the interaction of RIOK1 with RARRES1 inhibits its activity, resulting in p53 activation and subsequently to apoptosis induction. Consistent with this, knockdown of *RARRES1* in cultured podocyte reduced the TNFα-induced p53 phosphorylation and cleavage of caspase 3 (**Figure 5C**).

**Overexpression of RARRES1$^{WT}$, but not RARRES1$^{MT}$, induces proteinuria and podocyte loss in vivo**

We next examined the role of RARRES1 in vivo by inducing the podocyte-specific overexpression of wildtype RARRES1 or cleavage FFAF mutant in mice (RARRES1$^{WT}$ or RARRES1$^{MT}$ respectively, as described in **Figure S6**). The podocyte-specific expression of RARRES1$^{WT}$ and RARRES1$^{MT}$ was achieved by feeding the transgenic mice with doxycycline (Dox)-supplemented chow from 8 weeks to 20 weeks of age. Wildtype littermates fed with Dox chow were used as controls (RARRES$^{CL}$). All mice were sacrificed 20 weeks of age (12 weeks after Dox induction). RARRES1$^{WT}$ mice developed significant albuminuria, while RARRES1$^{CL}$ and RARRES1$^{MT}$ mice did not (**Figure 6A**). Consistent with this, RARRES1$^{WT}$ kidneys showed the development of glomerulosclerosis that was absent in the kidneys of RARRES1$^{CL}$ and RARRES1$^{MT}$ mice (**Figure 6B-C**). We did not detect significant change in BUN between all groups at 20 weeks of age. However, given the extent of glomerular injury in RARRES1$^{WT}$ mice, the renal function decline may become more significant in RARRES1$^{WT}$ mice at a later time point.

The ultrastructural analysis of podocyte foot processes showed significant effacement only in RARRES1$^{WT}$ mice at 20 weeks of age (**Figure 7A, 7C**). Moreover, quantification of WT-1+ cells also indicated a significant loss of podocytes in RARRES1$^{WT}$ mice, but not in RARRES1$^{CL}$ and RARRES1$^{MT}$ mice (**Figure 7B-C**). The TUNEL+ podocytes were more readily detected in the glomeruli of RARRES1$^{WT}$ mice, but not in those of RARRES1$^{CL}$ and RARRES1$^{MU}$ mice (**Figure 7B-C**). These results are consistent with the above in vitro results and indicate that the overexpression of RARRES1$^{WT}$ but not RARRES1$^{MT}$ induces podocyte loss through increased apoptosis.

**The knockdown of *Rarres1* attenuates albuminuria and glomerular injury in mice with Adriamycin-induced nephropathy.**

Given that the podocyte overexpression of RARRES1 induced glomerulosclerosis and proteinuria in vivo, we next examined whether the reduced RARRES1 expression might confer renoprotection in the setting of podocyte injury in vivo. We generated inducible podocyte-specific *Rarres1* knockdown mice as described in our previous study (23), and selected two independent lines with ~80-90% knockdown of RARRES1 expression for our studies, referred to as RARRES1$^{KD}$ (**Figure S7**). Knockdown of *Rarres1* was induced by feeding of Dox-supplemented chow, and wildtype littermates fed with Dox chow were used as controls (RARRES$^{CL}$). RARRES1$^{KD}$ mice did not develop albuminuria or any histological changes at the baseline up to the age of 6 months (data not shown). To establish Adriamycin (ADR)-induced nephropathy, RARRES1$^{KD}$ and RARRES1$^{CL}$ mice were first fed with Dox-supplemented chow starting at 6 weeks of age, and ADR was administered 2 weeks post Dox supplementation. All mice were sacrificed at 12 weeks of age. We found that RARRES1$^{KD}$ mice with ADR had attenuated albuminuria and glomerular injury when they were compared with RARRES1$^{CL}$ mice with ADR (**Figure 8A-D**). Quantification of WT1$^{+}$ and TUNEL$^{+}$ podocytes also indicated that RARRES1 knockdown led to the mitigation of podocyte loss and apoptosis in ADR mice (**Figure 8C-D**), confirming a role of RARRES1 in inducing podocyte injury in mice with experimental FSGS.

**DISCUSSION:**

In this study, utilizing the NEPTUNE datasets, we sought to determine the RA-related genes and signaling pathways in human glomerular disease. We found that many RA-related genes were highly regulated in human glomerular disease and correlated with the progression of kidney disease, further underscoring the importance of the RA signaling pathway in human glomerular disease. Interestingly, we found that several genes in the RA pathway, such as *RARRES1,* correlated positively with the progression of kidney disease, suggesting that although RA signaling largely confers renoprotection, as demonstrated in several experimental models (16, 17), few of the specific RA-induced downstream genes may concurrently elicit harmful effects in the kidney. Among these, we focused on *RARRES1*

for further analysis, because its expression correlated with the severity of human glomerular disease and predicted glomerular disease progression based on the NEPTUNE datasets. The correlation of increased glomerular expression of *RARRES1* with kidney disease was further corroborated by previously collected transcriptome datasets in patients with CKD and DKD and, together suggested that *RARRES1* is a risk gene for the progression of kidney disease. Interestingly, its mRNA expression in the recently published single-cell datasets (19-21) was shown to be largely limited to podocytes, a terminally differentiated and quiescent cell type in the glomeruli (1). RARRES1, whose role is implicated as a tumor suppressor (13, 14), may therefore contribute to podocyte quiescence in normal conditions.

We found TNF-α to be a potent inducer of RARRES1 expression in cultured podocytes and in turn RARRES1 mediates the pro-apoptotic effect of TNF-α in podocytes. Since TNF-α/NF-κB pathway is activated in diseased podocytes (24, 25), this is likely the main mechanism of increased RARRES1 expression in the diseased kidney. The role of TNFα in FSGS and DKD have been well demonstrated. Both circulating and local TNFα levels increase in patients with FSGS and DKD (25). A clinical trial using TNFα inhibitor for FSGS patients is ongoing (26). These findings together with our data suggest that either circulating or local TNFα, which is increased in FSGS or DKD, could induce RARRES1 expression and apoptosis in podocytes. Our in vitro data indicated that the overexpression of RARRES1 induces podocyte apoptosis by the activation of p53 pathway, and consistent with its previously reported tumor suppressor effect. We further validated in vivo that the overexpression of RARRES1 in podocytes alone is sufficient to induce albuminuria and podocyte loss in mice. Together, these in vitro and in vivo data suggest that high expression level of RARRES1 induces podocyte apoptosis and loss. Since podocyte loss is considered a major cause of progression of kidney disease including DKD and FSGS (2-4), the high expression level of RARRES1 likely contributes to the progression of DKD and FSGS.

A notable finding from our study is that the cleavage of RARRES1 is required for its pro-apoptotic function in cultured podocytes and that sequence flanking aa70 in its extracellular domain is a key cleavage site. *In silico* analysis suggests that this cleavage is mediated by a protease in the MMP family, and broad inhibition of MMPs reduced the cleavage of RARRES1. However, as there are 23 human MMPs with varying substrate specificities (27), future studies are required to dissect which MMPs are involved in the cleavage of RARRES1. Consistent with the in vitro data, the mice with overexpression of $RARRES1^{WT}$ in podocytes had soluble RARRES1 in the urine and developed albuminuria and podocyte loss, while the mice with overexpression of $RARRES1^{MT}$ in podocytes did not, further demonstrating that the cleavage of RARRES1 is required for its effect on podocyte loss in vivo. The utilization of $RARRES1^{MT}$ overexpression mice also served as a control for $RARRES1^{WT}$ overexpression mice, because of the concern of protein overexpression-induced cell toxicity.

Conversely, the knockdown of RARRES1 attenuates albuminuria and podocyte loss in mice with ADR-induced nephropathy, further supporting the role of RARRES1 in podocyte injury. Our data showed that knockdown of RARRES1 in podocytes did not cause any renal phenotype at the baseline, indicating that RARRES1 might not be essential or that the low amount of RARRES1 in these knockdown mice is sufficient to maintain normal podocyte function. Future studies are required to determine whether knockout of RARRES1 in podocytes causes any renal phenotype in mice, and whether soluble RARRES1 in the urine could be developed as a potential biomarker for progression of the glomerular disease.

Interestingly, the cleavage of RARRES1 and subsequent endocytic uptake of the soluble RARRES1 were required for the pro-apoptotic effect in cultured podocytes, indicating that RARRES1 likely needs to interact with intracellular signaling molecules to induce apoptosis. One such signaling molecule identified as an RARRES1-interacting protein was RIOK1. RIOK1 has been show to regulate cell survival and promote tumor growth, and the inhibition of RIOK1 is shown to induce apoptosis through the activation of p53 pathway (22, 28, 29). We confirmed that the apoptotic effect of RARRES1 was abolished when we overexpressed RIOK1, suggesting that RARRES1 interacts and suppresses RIOK1 function. Future studies are required to determine whether soluble RARRES1 promotes apoptosis in the neighboring cells such as glomerular endothelial cells or tubular cells via crosstalk mechanism. In addition, it would be informative to validate these new mechanisms in cancer cells.

Previous studies suggest that a low dose of RA induces podocytes differentiation (16, 30). However, our data showed that RA induced RARRES1 expression in a dose-dependent manner. These data suggest that while a low dose of RA might be beneficial, but a high dose of RA could be toxic for podocytes. It has been shown that the systemic adverse effects of RA are mediated by RA-induced apoptosis (31) and it would be interesting to determine whether RARRES1 also mediates the systemic adverse effects of RA. Therefore, we have to be cautious to consider RA as a drug to treat patients with glomerular disease. Our study also suggests that additional screening of drug-related pathways in human datasets could help the translation of the findings from animal studies to human disease.

In summary, we demonstrate a potentially novel mechanism by which RARRES1, a transmembrane protein acts on podocytes through releasing its cleaved form that subsequently interacts with an intracellular protein kinase to induce a pro-apoptotic effect, as summarized in **Figure 9**. Future studies are required to understand how the cleavage of RARRES1 is regulated in the diseased condition and inhibition of the cleavage could be an approach to target RARRES1 as a therapy for kidney disease and whether any genetic variants of RARRES1 are associated with glomerular disease.

## METHODS

Cell culture

HEK293T cells were obtained from ATCC (CRL-3216) and cultured according to their specifications. Conditionally immortalized human podocytes were obtained from Dr. Moin Saleem (Bristol, UK) and grown in RPMI-1640 medium supplemented with 10% fetal bovine serum, 1% penicillin-streptomycin, and 1x insulin-transferrin-selenite (ITS) media supplement (Sigma-Aldrich, St. Louis, MO). Podocytes were cultured on collagen I-coated plates and maintained at 33°C (5% $CO_2$, 90% humidity). Before experiments, cells were moved to 37 °C incubator and cultured for at least 5 days to fully induce differentiation. All experiments were repeated at least three times for each indicated condition. Podocytes between passages 9 and 20 were used in all experiments.

hRARRES1 wildtype and mutant protein expression

Human RARRES1 expression plasmids were constructed using the RARRES1 ORF (NM_206963). pTRE-Tight-hRARRES1 was constructed by ligating the hRARRES1 fragment into pTRE-Tight vector (Clontech: Cat.No.631059). FLAG-tagged RARRES1 expression plasmid (pTRE-Tight-FLAG-hRARRES1) was constructed by using the linker primers (F: 5'-GAATTCGACTACAAGGACGACGA TGACAAAGCCGG C-3'; R: 5'-GCCGGCTTTGTCATCGTCGTCCTTGTAG TCGAATTC-3'). N-terminal tagged human RARRES1 overexpression plasmid pCDNA4-FLAG-hRARRES1 was derived from pTRE-Tight-FLAG-hRARRES1 by subcloning the FLAG-hRARRES1 into pCDNA4 expression plasmid. C-terminal V5 tagged Human RARRES1 overexpression plasmid (pN1-hRARRES1-V5) was constructed in a similar manner. Primer linkers used to generate various V5-tagged RARRES1 plasmids are shown in **Table S5**. All constructs were verified with DNA sequencing.

Pull down and MS analysis

hRARRES1-V5 plasmid or control V5 plasmids was transfected to human podocyte cell lines with ViaFect™ transfection reagent (Promega, E4981). 36 hours post-transfection, the cells were harvested, total protein was extracted from the cell lysate with IP lysis buffer (Thermo Scientific, Prod# 87787) with protease inhibitor cocktail (Sigma P8340) and phosphatase inhibitor (Sigma P0044). The protein lysates were incubated with anti-V5-tag mAb-Magnetic beads (MBL, M167-11) at room temperature for 2 hours. Bound proteins after washing with IP lysis buffer were resuspended with 2X loading buffer and boiled for 2 minutes at 95℃. Protein gels were stained with Gel code blue stain reagent (Thermo Scientific #24590) for Mass spectrometry analysis. The protein identification using LC-MS/MS was performed at the Center for Advanced Proteomics Research Core at Rutgers New Jersey Medical School.

Flow cytometry analysis

Human podocytes were transfected with human RARRES1 overexpression plasmid with ViaFect™ transfection reagent (Promega, E4981). 36 hours post-transfection, cells were harvested and stained with Annexin V Apoptosis Detection Kit further (Thermo Fisher Scientific, 88-8007). The number of cells labeled with Annexin V-FITC and Propidium Iodide was quantified using the FACS Caliber Flow cytometer and the data were analyzed with CellQuest software (BD Biosciences).

TUNEL assay

The DeadEnd Colorimetric TUNEL System (Promega) was used to detect apoptotic cells on frozen kidney sections following the manufacturer's instructions. Cy5-conjugated streptavidin (Promega) was used to detect the apoptotic cells, and sections were then mounted with ProLong Gold Antifade Reagent with DAPI (Life Technologies).

Western Blot Analysis

Lysate preparation and Western blotting were performed according to the standard protocol. Each lane contained 30 to 60μg of total protein. Band density for the protein of interest was normalized to either GAPDH or β-actin. The following antibodies were used in this study: Human RARRES1 antibody (R&D AF4255), V5 (GenScript, Cat#: A01724), FLAG (Sigma, F3165), human RIOK1 (Abcam, ab176005), Cleaved Caspase-3 (Cell signal # 9664). Phospho-p53 (Ser46) (Cell Signaling #2521), pan-Cadherin (Invitrogen 71-7100), GAPDH (Cell Signaling, #2188), and β-actin (Sigma, A4700).

mRNA sequencing of cultured human podocytes

Total mRNA from cultured podocytes were harvested, sequenced, and analyzed as previously described (32). The data is deposited in NCBI's Gene Expression Omnibus (GEO) database (#GSE151484).

Quantitative Real-Time PCR

Real-time PCR was performed according to the standard protocol. Cycle threshold (Ct) values of the gene targets were normalized to GAPDH. Fold change in expression of target genes compared with the reference group was calculated using the 2-ΔΔCT method, with GAPDH as the calibrator. Sequences of primers used are as following: (hRARRES1) F: 5'-AGGTGTCACACTACTACTTGG-3', R: 5'-AGCTGTTGACAGTGGTACTTC-3'; (mRARRES1) F: 5'-TCGGCAGCTCATACGTGATGT-3', R: 5'-GTACCAGACCAAGTGAATACG-3'.

Preparation of the soluble human RARRES1

Human RARRES1 overexpression plasmid was transfected to 293T cells. At 12-hour post-transfection, the medium was changed to serum-free DMEM medium with 1% penicillin-streptomycin antibiotics. The supernatant was collected after 24 hours. The soluble RARRES1 was concentrated with amicon® ultra-15centrifugal filters (Millipore Sigma, C7715). The RARRES1 concentration was determined by the Enzyme-linked Immunosorbent Assay Kit for Retinoic Acid Receptor Responder 1 (RARRES1) of human RARRES1 (MyBioSource: MBS2019555). 10ng/mL soluble RARRES1 was was added into culture medium to treat podocytes.

Establishment of the inducible human wildtype and mutant RARRES1 overexpression mice and inducible RARRES1 knockdown mice:

The human RARRES1 cDNA was subcloned with the C-terminal V5 tag into into the inducible pTRE-Tight vector (Clontech, 631059). For the construction of the inducible mutant over-expression vectors, the purified fragment of the human mutant RARRES1 from previously constructed pN1-RARRES1(FFAF)-V5 vector was subcloned into the pTRE-Tight vector. The plasmids were digested with restriction enzymes to release the RARRES1-V5 encoding fragments for transgenic mouse derivation in surrogate FVB mice, generating the RARRES1 inducible mice (TRE-RARRES1$^{WT}$ or TRE-RARRES1$^{MT}$ mice). TRE-RARRES1 mice were crossed with *Nphs1*-rtTA mice (a gift from Dr. Jeffrey Miner, Washington University School of Medicine, St. Louis). The podocyte-specific expression of RARRES1 proteins was induced by the administration of doxycycline-supplemented chow (625g/kg, Envigo). For *Rarres1* knockdown mice, we used a similar protocol as described in our previous study (23). Briefly, TRE-*Rarres1* shRNA knockdown mice were obtained from Mirirus Inc. and crossed with *Nphs1*-rtTA mice to generate *Nphs1*-rtTA;TRE-*Rarres1*$^{KD}$ mice. Knockdown was induced with Dox chow as described above. Over-expression or knockdown of RARRES1 was verified by either qPCR or western blot analysis of isolated glomeruli from respective transgenic mice.

Mouse Kidney Histology

Kidney samples were fixed in 10% formalin, embedded in paraffin, and sectioned to 4-μm thickness. Periodic acid-Schiff (PAS)-stained kidney sections were used to examine the kidney histology. Histological scoring was performed in a blinded manner by the renal pathologist. Assessment of the mesangial and glomerular cross-sectional areas was performed by the operator blinded to the identity of the experimental groups by measuring the pixel counts on an average of a minimum of 10 glomeruli per section, under the 400x magnification (Zeiss AX10 microscope). Glomerulosclerosis was graded on a semi-quantitative scale (0 to 3+): 0 (absent), 1+ (involving 1%–25% of all glomeruli sampled), 2+ (involving 26%–50% of glomeruli), and 3+ (involving >50% of glomeruli) as described (17). An average of 25 glomeruli was sampled per animal were evaluated.

Transmission Electron Microscopy

Tissues were fixed in 2.5% glutaraldehyde with 0.1M sodium cacodylate (pH 7.4) for 72 hr at 4°C. Samples were further incubated with 2% osmium tetroxide and 0.1M sodium cacodylate (pH 7.4) for 1hr at room temperature. Ultrathin sections were stained with lead citrate and uranyl acetate and viewed on a Hitachi H7650 microscope. Briefly, negatives were digitized, and images with a final magnitude of up to X10,000 were obtained. ImageJ 1.26t software (National Institutes of Health, rsb.info.nih.gov) was used to measure the length of the peripheral GBM, and the number of slit pores overlying this GBM length was counted. The arithmetic mean of the foot process width ($W_{FP}$) was calculated as: $W_{FP} = \pi/4 \times (\sum_{GBM\ LENGTH})/(\sum_{silts})$,where $\Sigma_{slits}$ indicates the total number of slits counted; $\Sigma_{GBM\ LENGTH}$ indicates the total GBM length measured in one glomerulus, and $\pi/4$ is the correction factor for the random orientation by which the foot processes were sectioned (33).

Immunofluorescence

Mouse kidney tissues were harvested following the perfusion with 4% paraformaldehyde (PFA) in PBS, post-fixed for 2 hours on ice, equilibrated in 30% sucrose overnight, and frozen in OCT (Thermo Fisher Scientific) before sectioning. Kidney sections from human kidney biopsies were prepared accordingly. Then sections of 4μm were blocked with 2% horse serum and 2% BSA in PBS and incubated overnight at 4°C with the following primary antibodies: anti-RARRES1 (Santa Cruz, sc-390461), anti-NPSH2 antibody (Abcam, ab50339). Secondary antibodies conjugated with fluorochromes were obtained from Jackson Immuno-Research Labs. DAPI was used as a nuclear counterstain. Immunostained kidney sections were mounted with ProLong Gold Antifade Reagent with DAPI (Life Technologies).

Immunohistochemistry

Formalin-fixed and paraffin-embedded sections were deparaffinized, and endogenous peroxidase was inactivated with $H_2O_2$. Sections were then blocked in 2% goat serum in phosphate-buffered saline (PBS) for 1 hour at room temperature and then incubated with anti-RARRES1 (Santa Cruz, sc-390461) at 4°C overnight. The next day, sections were washed three times with PBS and then incubated with secondary antibody for 30 minutes. Positive staining was revealed by peroxidase-labeled streptavidin and diaminobenzidine substrate with a fixed exposure time of 3 minutes for all experiments among the groups. The control included a section stained with only secondary antibody.

Quantification of Immunostaining

Immunostained images with a final magnitude of approximately X400 were obtained. ImageJ 1.26t software was used to measure the level of immunostaining in the glomeruli. First, the images were

converted to 8-bit grayscale. Glomerular regions were selected for measurement of area and integrated density, and background intensity was measured by selecting three distinct areas in the background with no staining. The corrected optical density (COD) was determined as shown below:

$$\mathbf{COD} = \boldsymbol{ID} - (\boldsymbol{A} \times \boldsymbol{MGV})$$

where ID is the integrated density of the selected glomerular region, A is the area of the selected glomerular region, and MGV is the mean gray value of the background readings (34).

Statistical Analysis

Data are expressed as mean±SD or SEM as indicated. Unpaired, two-tailed t-test was used to analyze data between two groups. 1-way or 2-way ANOVA with Tukey's multiple comparison test was used when more than two groups were present, as indicated. All experiments were repeated at least three times, and representative experiments are shown. Statistical significance was achieved when $p < 0.05$.

Study Approval

The human kidney biopsy sample collection was approved by the Medical Ethics Committee of Zhongshan Hospital affiliated to Xiamen University (2020-054). All animal procedures were performed according to protocols approved by the Institutional Animal Care and Use Committee at the Icahn School of Medicine at Mount Sinai (IACUC# 06-1098).

## AUTHOR CONTRIBUTIONS

A.C., K.L, J.C.H. designed and conducted experiments, acquired and analyzed data, and wrote MS; Y.F, H.L., J.W., Z.L., Y.L, A.W, Q.H., F.Z., C.W., J.F., T.G., B.L, M.K., acquired and analyzed data.


## ACKNOWLEDGMENTS

AQC is supported by the National Natural Science Foundation of China (grant no.81800637), Natural Science Foundation of Fujian Province (2019J01560) and Xiamen Science and Technology Project (grant no. 3502Z20194014). JCH is supported by VA Merit Award IBX000345C, NIH 1R01DK078897, NIH 1R01DK088541, and NIH P01DK56492. KL is supported by NIH R01DK117913.


## CONFLICT OF INTEREST:

The authors declare that they have no competing financial interests.

## REFERENCES

1. Durvasula RV, and Shankland SJ. Podocyte injury and targeting therapy: an update. *Current opinion in nephrology and hypertension.* 2006;15(1):1-7.

2. Pagtalunan ME, Miller PL, Jumping-Eagle S, Nelson RG, Myers BD, Rennke HG, et al. Podocyte loss and progressive glomerular injury in type II diabetes. *J Clin Invest.* 1997;99(2):342-8.

3. Steffes MW, Schmidt D, McCrery R, and Basgen JM. Glomerular cell number in normal subjects and in type 1 diabetic patients. *Kidney Int.* 2001;59(6):2104-13.

4. Nishizono R, Kikuchi M, Wang SQ, Chowdhury M, Nair V, Hartman J, et al. FSGS as an Adaptive Response to Growth-Induced Podocyte Stress. *J Am Soc Nephrol.* 2017;28(10):2931-45.

5. Tharaux PL, and Huber TB. How many ways can a podocyte die? *Semin Nephrol.* 2012;32(4):394-404.

6. Evans TR, and Kaye SB. Retinoids: present role and future potential. *Br J Cancer.* 1999;80(1-2):1-8.

7. Okuno M, Kojima S, Matsushima-Nishiwaki R, Tsurumi H, Muto Y, Friedman SL, et al. Retinoids in cancer chemoprevention. *Current cancer drug targets.* 2004;4(3):285-98.

8. Xu Q, Lucio-Cazana J, Kitamura M, Ruan X, Fine LG, and Norman JT. Retinoids in nephrology: promises and pitfalls. *Kidney Int.* 2004;66(6):2119-31.

9. Mallipattu SK, and He JC. The beneficial role of retinoids in glomerular disease. *Front Med (Lausanne).* 2015;2:16.

10. Montesinos P, Bergua JM, Vellenga E, Rayon C, Parody R, de la Serna J, et al. Differentiation syndrome in patients with acute promyelocytic leukemia treated with all-trans retinoic acid and anthracycline chemotherapy: characteristics, outcome, and prognostic factors. *Blood.* 2009;113(4):775-83.

11. Piersma AH, Hessel EV, and Staal YC. Retinoic acid in developmental toxicology: Teratogen, morphogen and biomarker. *Reproductive toxicology.* 2017;72:53-61.

12. Nagpal S, Patel S, Asano AT, Johnson AT, Duvic M, and Chandraratna RA. Tazarotene-induced gene 1 (TIG1), a novel retinoic acid receptor-responsive gene in skin. *The Journal of investigative dermatology.* 1996;106(2):269-74.

13. Sahab ZJ, Hall MD, Zhang L, Cheema AK, and Byers SW. Tumor Suppressor RARRES1 Regulates DLG2, PP2A, VCP, EB1, and Ankrd26. *Journal of Cancer.* 2010;1:14-22.

14. Oldridge EE, Walker HF, Stower MJ, Simms MS, Mann VM, Collins AT, et al. Retinoic acid represses invasion and stem cell phenotype by induction of the metastasis suppressors RARRES1 and LXN. *Oncogenesis.* 2013;2:e45.

15. Gadegbeku CA, Gipson DS, Holzman LB, Ojo AO, Song PX, Barisoni L, et al. Design of the Nephrotic Syndrome Study Network (NEPTUNE) to evaluate primary glomerular nephropathy by a multidisciplinary approach. *Kidney Int.* 2013;83(4):749-56.

16. He JC, Lu TC, Fleet M, Sunamoto M, Husain M, Fang W, et al. Retinoic acid inhibits HIV-1-induced podocyte proliferation through the cAMP pathway. *J Am Soc Nephrol.* 2007;18(1):93-102.

17. Ratnam KK, Feng X, Chuang PY, Verma V, Lu TC, Wang J, et al. Role of the retinoic acid receptor-alpha in HIV-associated nephropathy. *Kidney Int.*79(6):624-34.

18. Woroniecka KI, Park AS, Mohtat D, Thomas DB, Pullman JM, and Susztak K. Transcriptome analysis of human diabetic kidney disease. *Diabetes.* 2011;60(9):2354-69.

19. Park J, Shrestha R, Qiu C, Kondo A, Huang S, Werth M, et al. Single-cell transcriptomics of the mouse kidney reveals potential cellular targets of kidney disease. *Science.* 2018;360(6390):758-63.

20. Karaiskos N, Rahmatollahi M, Boltengagen A, Liu H, Hoehne M, Rinschen M, et al. A Single-Cell Transcriptome Atlas of the Mouse Glomerulus. *J Am Soc Nephrol.* 2018;29(8):2060-8.

21. Fu J, Akat KM, Sun Z, Zhang W, Schlondorff D, Liu Z, et al. Single-Cell RNA Profiling of Glomerular Cells Shows Dynamic Changes in Experimental Diabetic Kidney Disease. *J Am Soc Nephrol.* 2019;30(4):533-45.

22. Read RD, Fenton TR, Gomez GG, Wykosky J, Vandenberg SR, Babic I, et al. A kinome-wide RNAi screen in Drosophila Glia reveals that the RIO kinases mediate cell proliferation and survival through TORC2-Akt signaling in glioblastoma. *PLoS genetics.* 2013;9(2):e1003253.

23. Chuang PY, Xu J, Dai Y, Jia F, Mallipattu SK, Yacoub R, et al. In vivo RNA interference models of inducible and reversible Sirt1 knockdown in kidney cells. *Am J Pathol.* 2014;184(7):1940-56.

24. Wiggins JE, Patel SR, Shedden KA, Goyal M, Wharram BL, Martini S, et al. NFkappaB promotes inflammation, coagulation, and fibrosis in the aging glomerulus. *J Am Soc Nephrol.* 2010;21(4):587-97.

25. Pedigo CE, Ducasa GM, Leclercq F, Sloan A, Mitrofanova A, Hashmi T, et al. Local TNF causes NFATc1-dependent cholesterol-mediated podocyte injury. *J Clin Invest.* 2016;126(9):3336-50.

26. Joy MS, Gipson DS, Powell L, MacHardy J, Jennette JC, Vento S, et al. Phase 1 trial of adalimumab in Focal Segmental Glomerulosclerosis (FSGS): II. Report of the FONT (Novel Therapies for Resistant FSGS) study group. *American journal of kidney diseases : the official journal of the National Kidney Foundation.* 2010;55(1):50-60.

27. Nagase H, Visse R, and Murphy G. Structure and function of matrix metalloproteinases and TIMPs. *Cardiovasc Res.* 2006;69(3):562-73.

28. Zhang T, Ji D, Wang P, Liang D, Jin L, Shi H, et al. The atypical protein kinase RIOK3 contributes to glioma cell proliferation/survival, migration/invasion and the AKT/mTOR signaling pathway. *Cancer letters.* 2018;415:151-63.

29. Weinberg F, Reischmann N, Fauth L, Taromi S, Mastroianni J, Kohler M, et al. The Atypical Kinase RIOK1 Promotes Tumor Growth and Invasive Behavior. *EBioMedicine.* 2017;20:79-97.

30. Vaughan MR, Pippin JW, Griffin SV, Krofft R, Fleet M, Haseley L, et al. ATRA induces podocyte differentiation and alters nephrin and podocin expression in vitro and in vivo. *Kidney Int.* 2005;68(1):133-44.

31. Melnik BC. Overexpression of p53 explains isotretinoin's teratogenicity. *Experimental dermatology.* 2018;27(1):91-3.

32. Fu J, Wei C, Zhang W, Schlondorff D, Wu J, Cai M, et al. Gene expression profiles of glomerular endothelial cells support their role in the glomerulopathy of diabetic mice. *Kidney Int.* 2018;94(2):326-45.

33. Koop K, Eikmans M, Baelde HJ, Kawachi H, De Heer E, Paul LC, et al. Expression of podocyte-associated molecules in acquired human kidney diseases. *J Am Soc Nephrol.* 2003;14(8):2063-71.

34. Potapova TA, Sivakumar S, Flynn JN, Li R, and Gorbsky GJ. Mitotic progression becomes irreversible in prometaphase and collapses when Wee1 and Cdc25 are inhibited. *Mol Biol Cell.* 2011;22(8):1191-206.

32. Ratnam KK, et al. Role of the retinoic acid receptor-α in HIV-associated nephropathy. Kidney Int. 2011;79(6):624–634

| Symbol | Identified Proteins | Ratio |
|---|---|---|
| GTF3C1 | General transcription factor 3C polypeptide 1 OS=Homo sapiens GN=GTF3C1 PE=1 SV=4 | 76.5 |
| ZNF318 | Zinc finger protein 318 OS=Homo sapiens GN=ZNF318 PE=1 SV=2 | 66 |
| KHDRBS1 | KH domain-containing, RNA-binding, signal transduction-associated protein 1 OS=Homo sapiens GN=KHDRBS1 PE=1 SV=1 | 49 |
| **RIOK1** | **Serine/threonine-protein kinase RIO1 OS=Homo sapiens GN=RIOK1 PE=1 SV=2** | **46.5** |
| NVL | Nuclear valosin-containing protein-like OS=Homo sapiens GN=NVL PE=1 SV=1 | 43.5 |
| MYCBP2 | E3 ubiquitin-protein ligase MYCBP2 OS=Homo sapiens GN=MYCBP2 PE=1 SV=3 | 43 |
| GTF2I | General transcription factor II-I OS=Homo sapiens GN=GTF2I PE=1 SV=2 | 42.6 |
| SUPT16H | FACT complex subunit SPT16 OS=Homo sapiens GN=SUPT16H PE=1 SV=1 | 40.7 |
| GTF3C4 | General transcription factor 3C polypeptide 4 OS=Homo sapiens GN=GTF3C4 PE=1 SV=2 | 38.5 |
| GTF3C3 | General transcription factor 3C polypeptide 3 OS=Homo sapiens GN=GTF3C3 PE=1 SV=1 | 37 |

**Table 1: Top 10 RARRES1-interacting proteins identified by IP-MS.**

**Figure legends:**

**Figure 1: *RARRES1* mRNA expression correlates with clinical outcomes.** (A) The association of glomerular RARRES1 expression level with eGFR slope of the CKD cohort in the NEPTUNE dataset. (B) Cumulative survival by tertiles of RARRES1 gene expression level (Kaplan–Meier analysis). The lowest tertile correspond to RARRES1 gene expression lower than 3.103, middle tertile between 3.103-3.857, and the highest tertile greater than 3.857. Twenty seven out of 152 patients progressed to composite endpoint of ESRD or 40% baseline eGFR reduction.

**Figure 2: RARRES1 expression increased in FSGS and DKD.** (A) The Immunohistochemical staining of RARRES1 in human renal biopsy specimens. Isotype IgG was used for negative control. MCD, minimal change disease; FSGS, focal glomerulosclerosis; DKD, diabetic kidney disease. Scale bar: 50μm. (B) Quantification of mean RARRES1 intensity per glomerular cross section for human renal biopsy specimens as a fold change relative to MCD (n=5 specimens per group, 10 glomeruli evaluated for each specimen). Data represent mean±SD, **P<0.01 and ****P<0.0001 vs. MCD; $^{###}$P<0.001 vs. FSGS by 1-way ANOVA with Tukey's multiple comparison test. (C) Immunofluorescence co-staining of RARRES1 and Podocin in renal biopsy specimen of DKD patients. Scale bar: 20μm.

**Figure 3: RARRES1 is cleaved and released into the supernatants as a highly glycosylated soluble form.** (A) Cultured human podocytes were transiently transfected to express control EGFP or C-terminal V5-tagged RARRES1 (RARRES1-V5). Expression of RARRES1 was probed with V5 antibody in the cytoplasmic (C) and membrane (M) fractions in comparison to the total cell lysate (T). Pan-Cadherin was used to confirm the membrane protein enrichment in the M fraction. (B) Total cell lysate (CL) or supernatant (Supe) from cultured podocytes expressing control EGFP or C-terminal V5-tagged RARRES1 (RARRES1-V5) was probed for RARRES1 expression using V5 antibody. (C) Total cell lysate (CL) or supernatant (Supe) from cultured podocytes expressing control EGFP or N-terminal FLAG-tagged RARRES1 (FLAG-RARRES1) was probed for RARRES1 expression using FLAG antibodies. (D) Total cell lysate (CL) or supernatant (Supe) from cultured podocytes expressing RARRES1-V5 with or without deglycosylation treatment were probed with V5 antibody. Arrowheads indicate the shift in the RARRES1-V5 migration with or without deglycosylation. (E) Total cell lysate (CL) or supernatant (Supe) from cultured podocytes expressing EGFP control, C-terminal V5 tagged RARRES1 with the deletion of aa43-76 (Δaa43-76-V5), deletion of aa43-55 (Δaa43-55-V5), or wildtype RARRES1 (RARRES1-V5) was probed with V5 and RARRES1 antibodies. (F) Supernatant from cultured podocytes expressing C-terminal V5-tagged RARRES1 with the deletion of aa68-71 (ΔFFNF-V5), alanine substitution of individual amino acids of aa68-71 as indicated in underlined A

residue (AAAA-V5, AFNF-V5, FANF-V5, FFAF-V5, and FFNA-V5), aspartic acid substitution of aa70 (FFDF-V5), or wildtype RARRES1 (RARRES1-V5) was probed for expression with V5 antibody. (G) Total cell lysate (CL) or supernatant (Supe) from cultured podocytes expressing EGFP control, C-terminal V5-tagged RARRES1 (RARRES1-V5) or RARRES1 FFAF mutant (FFAF-V5) with or without the treatment of broad spectrum MMP inhibitor, Marimastat (50μM) were probed with V5 antibody. (H) Total cell lysate (CL), supernatant (Supe), or isolated ectosomes (Ecto) from cultured podocytes expressing EGFP control, C-terminal V5-tagged RARRES1 (RARRES1-V5) or RARRES1 FFAF mutant (FFAF-V5) was probed with V5 antibody.

**Figure 4: Blockade of RARRES1 cleavage mitigates the apoptotic potential of RARRES1 overexpression in cultured human podocytes.** (A) Apoptosis assay on cultured podocytes expressing control EGFP, wildtype RARRES1 (RARRES1-V5), or RARRES1 cleavage mutant (FFAF-V5) at 24 hours post-transfection by flow cytometry for Annexin V and propidium iodide (PI). (B) Western blot analysis of cleaved Caspase-3 (arrowhead) in transfected cells in (A). (C) Annexin V flow cytometry assay on cultured podocytes incubated with soluble RARRES1 (sRARRES1-V5, 10ng/mL, 24 hours of incubation) from supernatant of HEK293T cells overexpressing RARRES1-V5. (D) Western blot analysis of cleaved caspase-3 in podocytes in (C). (E) Human podocytes were incubated with 10ng/ml sRARRES1-V5 with or without endocytosis inhibitor Dynasore (80μM) for 1 hour and total cell lysates were immunoblotted with V5 antibody. (F) Human podocytes were incubated with 10ng/ml sRARRES1-V5 with or without a lower dose of Dynasore (10μM) for 12 hours. Lysates were probed with V5 and cleaved Caspase-3 (Cl-Casp3) antibodies.

**Figure 5: RIOK interacts with RARRES1 and TNFα induces apoptosis through RARRES1 and RIOK1**. (A) Podocytes were co-transfected with myc-DDK-tagged RIOK1 (RIOK1-myc-DDK) with either control EGFP vector, wildtype RARRES1-V5, or cleavage mutant FFAF-V5. Lysates were immunoprecipitated with V5 antibody to pull down the RARRES1-interacting proteins and probed with FLAG and RIOK-1 antibodies. Input lysates were probed with FLAG, RIOK1, V5, and GAPDH antibodies. (B) Human podocytes were transfected with overexpression plasmids of RARRES1-V5 and/or RIOK1-myc-DDK. Western blot analysis was performed 24 hours post transfection for phospho-p53 (ser46), cleaved Caspase-3, and RARRES1. (C) Podocytes stably transduced with lentiviral vector expressing scrambled control shRNA or *RARRES1* shRNA were treated with TNF-α (10 ng/ml for 24 hours). Lysates were probed for p-p53 (Ser46), RARRES1, and cleaved Caspase-3. The representative blots of three independent experiments are shown.

**Figure 6: Podocyte overexpression of RARRES$^{WT}$ induces glomerular injury.** (A) 24-hour albumin excretion. (B) Representative images of PAS-stained kidneys. Scale bars, 50μm (upper panel), 20μm (lower panel). (C) Average glomerulosclerosis (GS) score per glomerular cross section per mouse (n=6 mice per group, 25 glomeruli evaluated for each mouse, Data represents mean±SD).****P<0.0001 vs. RARRES1$^{CL}$; ####P<0.0001 vs. RARRES1$^{WT}$ by 1-way ANOVA with Tukey's multiple comparison test.

**Figure 7: Podocyte overexpression of RARRES$^{WT}$ induces podocyte injury and loss.** (A) Representative transmission EM images for low and high magnifications. Scale bars, 1μm. (B) Representative images of WT1 immunostaining (red) and TUNEL staining (green). Scale bars, 20μm. Arrowhead shows the WT1+ and TUNEL+ cell in RARRES$^{WT}$ kidney and magnified view is shown in the dotted inset. (C) Quantification of average foot process (n=4 mice per group evaluated) from TEM images (n=4 mice per group) and average TUNEL+ and WT1+ cells per glomerular cross section (gcs) per mouse (n=6 mice per group, 10 glomeruli evaluated for each mouse. All data represent mean±SD. ****P<0.0001 vs. RARRES1$^{CL}$; ###P<0.001 and ####P<0.0001 vs. RARRES1$^{WT}$ by 1-way ANOVA with Tukey's multiple comparison test.

**Figure 8: Podocyte *Rarres1* knockdown attenuates albuminuria and glomerular injury in Adriamycin (ADR)-induced nephropathy in mice.** *Nphs1*-rtTA;TRE-*Rarres1*$^{KD}$ mice were given either control chow (RARRES1$^{CL}$) or Dox-supplemented chow (RARRES1$^{KD}$) for two weeks prior to ADR (+ADR) or vehicle (-ADR) injection. All mice were sacrificed after 4 weeks post injection. (A) UACR after ADR or vehicle injection, where week 0 indicates the baseline prior to injection. Data represent mean±SEM, n=5 mice per group. **P<0.01, ***P<0.001, and ****P<0.0001 vs. respective -ADR control; ####P<0.0001 vs. RARRES1$^{CL}$+ADR by 2-way ANOVA with Tukey's multiple comparison test. (B) Representative images of PAS-stained kidneys. Original magnification, x200 (upper panels, x400 (lower panels), Scale bar, 20μm. (C) Representative images of WT1 (red) and TUNEL (green) co-immunostaining. Scale bars, 20μm. A magnified view of WT1+ and TUNEL+ cell is shown in the inset. (D) Average glomerulosclerosis (GS) score per glomerular cross section per mouse (n=5 mice per group, 25 glomeruli evaluated for each mouse) and TUNEL+ and WT1+ cells per glomerular cross section (gcs) per mouse (n=5 mice per group, 15 glomeruli evaluated for each mouse). Data represent mean±SD, ***P<0.001 and ****P<0.0001 vs. -ADR control; ##P<0.01 and ####P<0.0001 vs. RARRES1$^{CL}$+ADR by 1-way ANOVA with Tukey's multiple comparison test.

**Figure 9: Summary of the mechanism by which RARRES1 regulates podocyte apoptosis.** TNFα induces expression of RARRES1, which is cleaved into soluble RARRES1, potentially mediated by inflammation-stimulated MMP. The soluble RARRES1 is then endocytosed and interacts with

intracellular RIOK1. The interaction between RIOK1 and RARRES1 leads to the inactivation of RIOK1, thereby activating p53 and apoptosis pathway. Podocyte loss is a key event for progression of DKD and FSGS.

## Figure 1

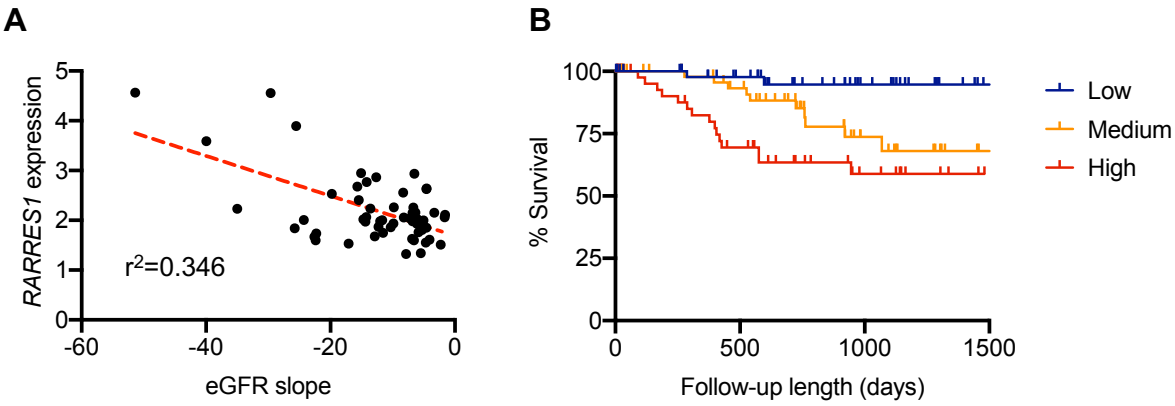


**Figure 1: *RARRES1* mRNA expression correlates with clinical outcomes.** (A) The association of glomerular *RARRES1* expression level with eGFR slope of the CKD cohort in the NEPTUNE dataset. (B) Cumulative survival by tertiles of *RARRES1* gene expression level (Kaplan–Meier analysis). The lowest tertile correspond to *RARRES1* gene expression lower than 3.103, middle tertile between 3.103-3.857, and the highest tertile greater than 3.857. Twenty seven out of 152 patients progressed to composite endpoint of ESRD or 40% baseline eGFR reduction.

## Figure 2

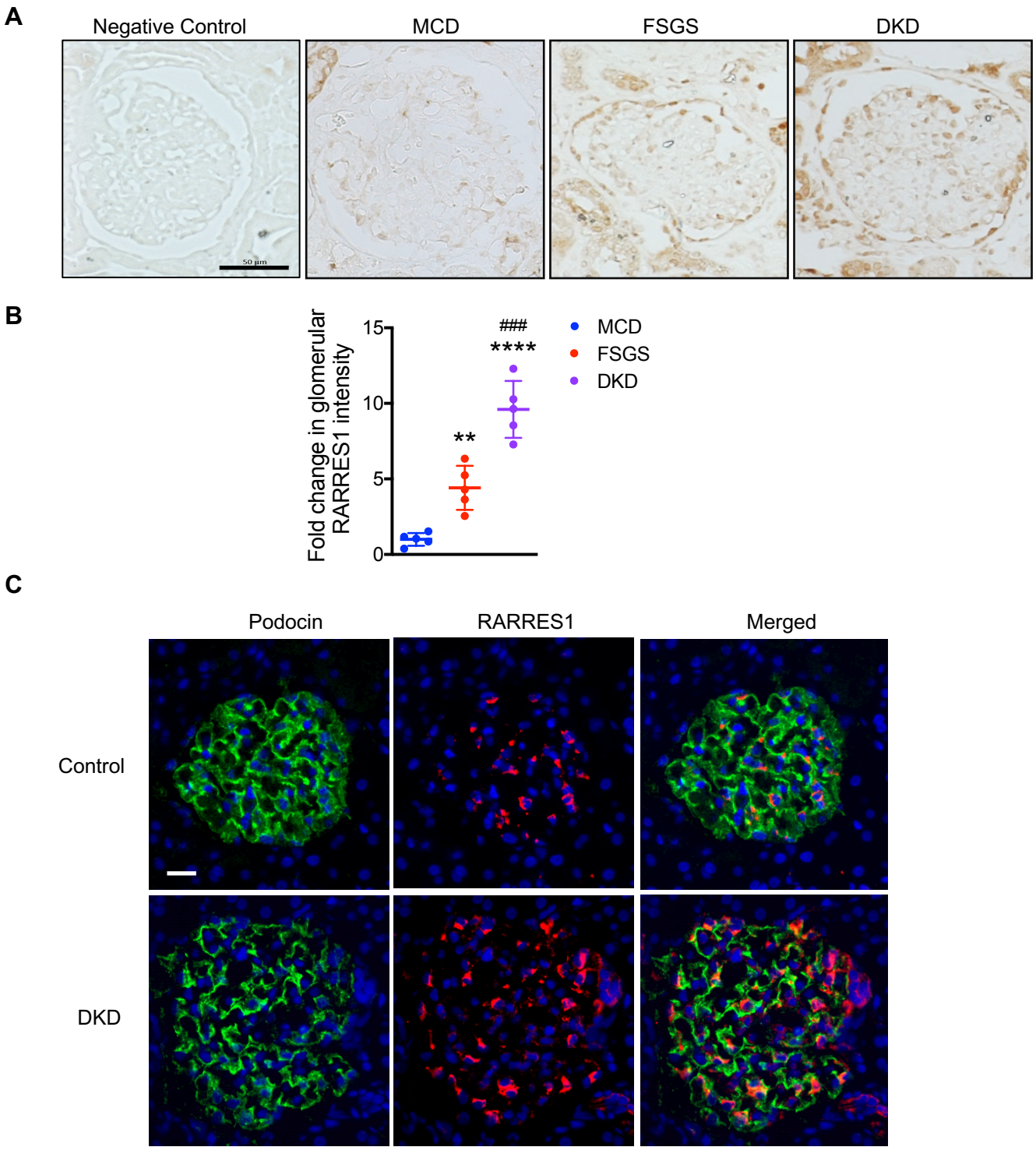


**Figure 2: RARRES1 expression increased in DKD.** (A) The Immunohistochemical staining of RARRES1 in human renal biopsy specimens. Isotype IgG was used for negative control. MCD, minimal change disease; FSGS, focal glomerulosclerosis; DKD, diabetic kidney disease. Scale bar: 50μm. (B) Quantification of mean RARRES1 intensity per glomerular cross section for human renal biopsy specimens as a fold change relative to MCD (n=5 specimens per group, 10 glomeruli evaluated for each specimen). Data represent mean±SD, **P<0.01 and ****P<0.0001 vs. MCD; ###P<0.001 vs. FSGS by 1-way ANOVA with Tukey's multiple comparison test. (C) Immunofluorescence co-staining of RARRES1 and Podocin in renal biopsy specimen of DKD patients. Scale bar: 20μm.

**Figure 3**

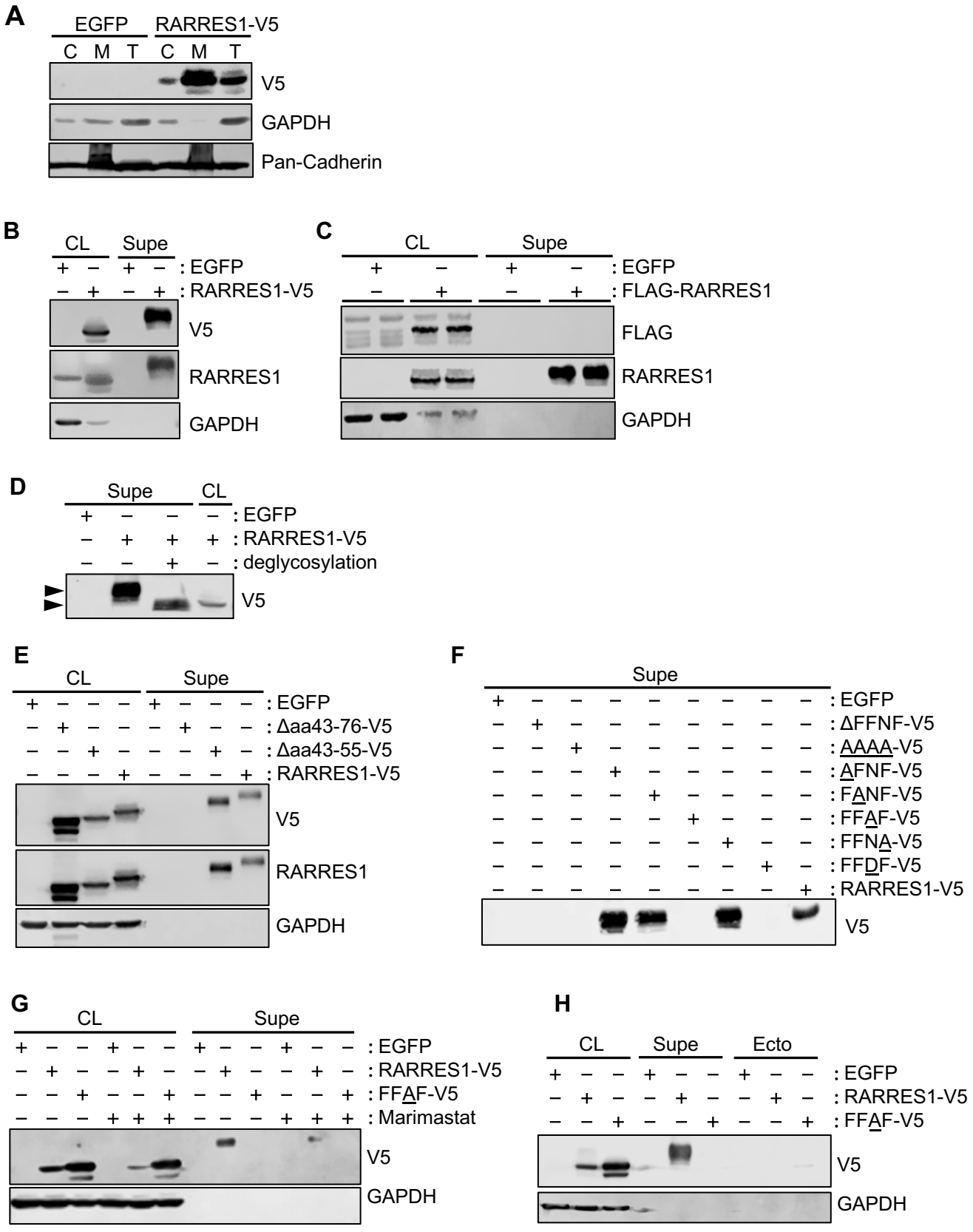
A
EGFP
RARRES1-V5
C M T C M T
V5
GAPDH
Pan-Cadherin
B
CL
Supe
+ − + − : EGFP
− + − + : RARRES1-V5
V5
RARRES1
GAPDH
C
CL
Supe
+ − + − : EGFP
− + − + : FLAG-RARRES1
FLAG
RARRES1
GAPDH
D
Supe
CL
+ − − − : EGFP
− + + + : RARRES1-V5
− − + − : deglycosylation
V5
E
CL
Supe
+ − − − + − − − : EGFP
− + − − − + − − : Δaa43-76-V5
− − + − − − + − : Δaa43-55-V5
− − − + − − − + : RARRES1-V5
V5
RARRES1
GAPDH
F
Supe
+ − − − − − − − − : EGFP
− + − − − − − − − : ΔFFNF-V5
− − + − − − − − − : AAAA-V5
− − − + − − − − − : AFNF-V5
− − − − + − − − − : FANF-V5
− − − − − + − − − : FFAF-V5
− − − − − − + − − : FFNA-V5
− − − − − − − + − : FFDF-V5
− − − − − − − − + : RARRES1-V5
V5
G
CL
Supe
+ − − + − − + − − + − − : EGFP
− + − − + − − + − − + − : RARRES1-V5
− − + − − + − − + − − + : FFAF-V5
− − − + + + − − − + + + : Marimastat
V5
GAPDH
H
CL
Supe
Ecto
+ − − + − − + − − : EGFP
− + − − + − − + − : RARRES1-V5
− − + − − + − − + : FFAF-V5
V5
GAPDH

**Figure 3: RARRES1 is cleaved and released into the supernatants as a highly glycosylated soluble form.** (A) Cultured human podocytes were transiently transfected to express control EGFP or C-terminal V5-tagged RARRES1 (RARRES1-V5). Expression of RARRES1 was probed with V5 antibody in the cytoplasmic (C) and membrane (M) fractions in comparison to the total cell lysate (T). Pan-Cadherin was used to confirm the membrane protein enrichment in the M fraction. (B) Total cell lysate (CL) or supernatant (Supe) from cultured podocytes expressing control EGFP or C-terminal V5-tagged RARRES1 (RARRES1-V5) was probed for RARRES1 expression using V5 antibody. (C) Total cell lysate (CL) or supernatant (Supe) from cultured podocytes expressing control EGFP or N-terminal FLAG-tagged RARRES1 (FLAG-RARRES1) was probed for RARRES1 expression using FLAG antibodies. (D) Total cell lysate (CL) or supernatant (Supe) from cultured podocytes expressing RARRES1-V5 with or without deglycosylation treatment were probed with V5 antibody. Arrowheads indicate the shift in the RARRES1-V5 migration with or without deglycosylation. (E) Total cell lysate (CL) or supernatant (Supe) from cultured podocytes expressing EGFP control, C-terminal V5 tagged RARRES1 with the deletion of aa43-76 (Δaa43-76-V5), deletion of aa43-55 (Δaa43-55-V5), or wildtype RARRES1 (RARRES1-V5) was probed with V5 and RARRES1 antibodies. (F) Supernatant from cultured podocytes expressing C-terminal V5-tagged RARRES1 with the deletion of aa68-71 (ΔFFNF-V5), alanine substitution of individual amino acids of aa68-71 as indicated in underlined A residue (AAAA-V5, AFNF-V5, FANF-V5, FFAF-V5, and FFNA-V5), aspartic acid substitution of aa70 (FFDF-V5), or wildtype RARRES1 (RARRES1-V5) was probed for expression with V5 antibody. (G) Total cell lysate (CL) or supernatant (Supe) from cultured podocytes expressing EGFP control, C-terminal V5-tagged RARRES1 (RARRES1-V5) or RARRES1 FFAF mutant (FFAF-V5) with or without the treatment of broad spectrum MMP inhibitor, Marimastat (50mM) were probed with V5 antibody. (H) Total cell lysate (CL), supernatant (Supe), or isolated ectosomes (Ecto) from cultured podocytes expressing EGFP control, C-terminal V5-tagged RARRES1 (RARRES1-V5) or RARRES1 FFAF mutant (FFAF-V5) was probed with V5 antibody.

**Figure 4**

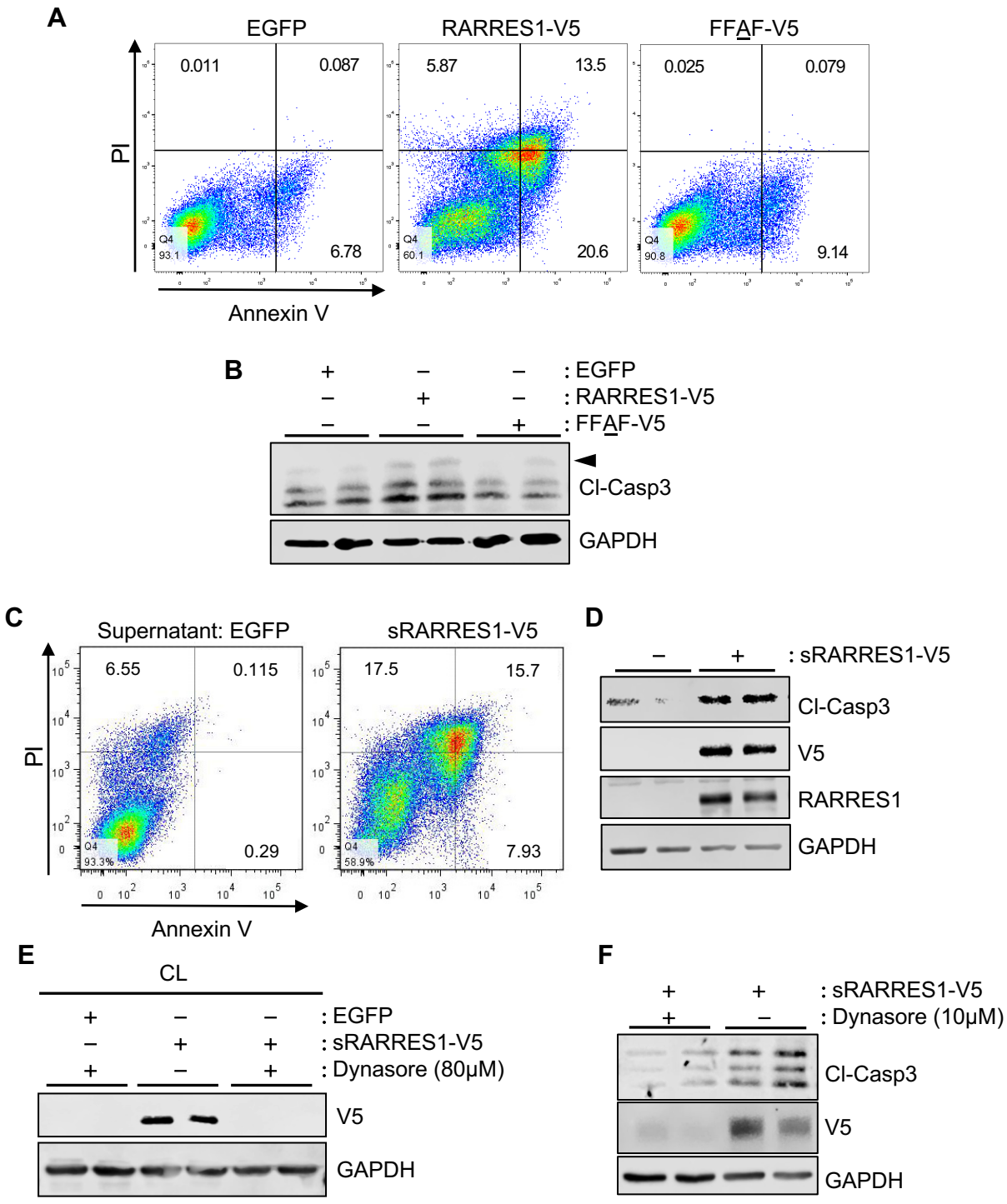


**Figure 4: Blockade of RARRES1 cleavage mitigates the apoptotic potential of RARRES1 overexpression in cultured human podocytes.** (A) Apoptosis assay on cultured podocytes expressing control EGFP, wildtype RARRES1 (RARRES1-V5), or RARRES1 cleavage mutant (FFAF-V5) at 24 hours post-transfection by flow cytometry for Annexin V and propidium iodide (PI). (B) Western blot analysis of cleaved Caspase-3 (arrowhead) in transfected cells in (A). (C) Annexin V flow cytometry assay on cultured podocytes incubated with soluble RARRES1 (sRARRES1-V5, 10ng/mL, 24 hours of incubation) from supernatant of HEK293T cells overexpressing RARRES1-V5. (D) Western blot analysis of cleaved caspase-3 in podocytes in (C). (E) Human podocytes were incubated with 10ng/ml sRARRES1-V5 with or without endocytosis inhibitor Dynasore (80mM) for 1 hour and total cell lysates were immunoblotted with V5 antibody. (F) Human podocytes were incubated with 10ng/ml sRARRES1-V5 with or without a lower dose of Dynasore (10mM) for 12 hours. Lysates were probed with V5 and cleaved Caspase-3 (Cl-Casp3) antibodies.

## Figure 5

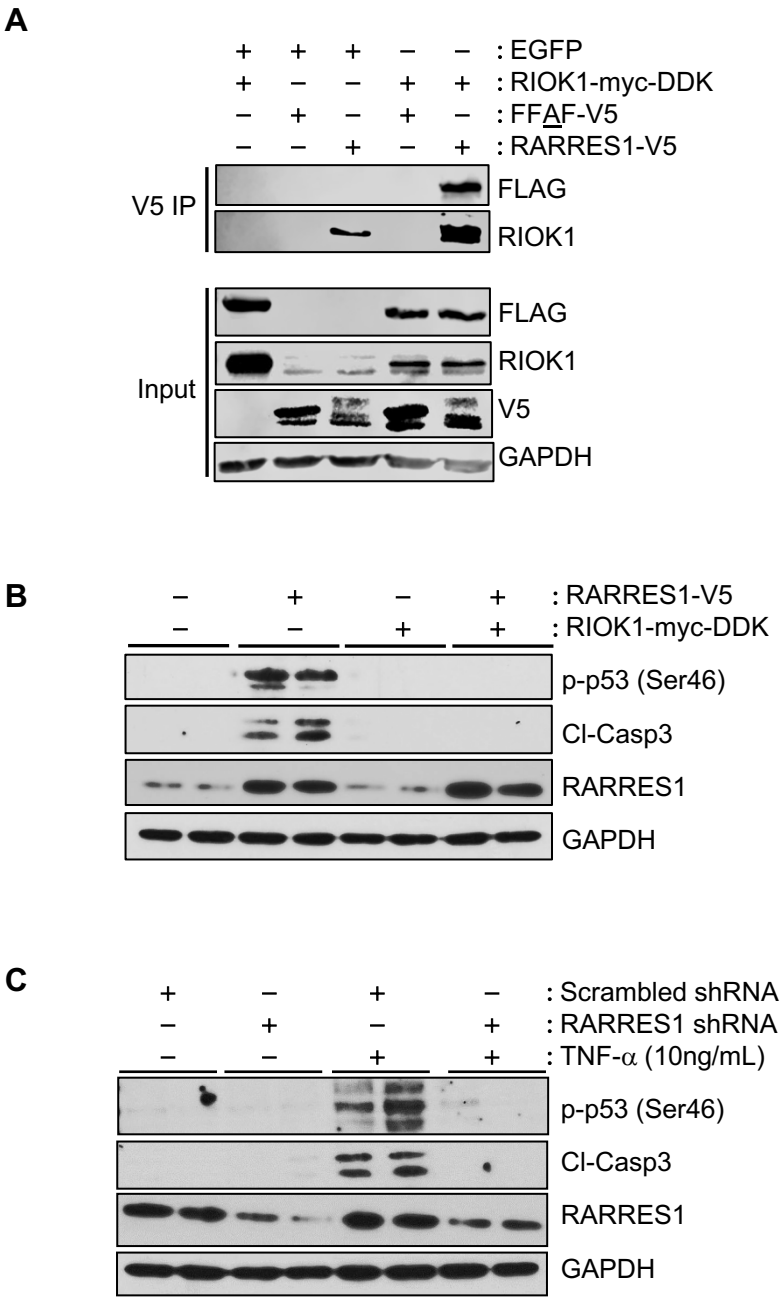


**Figure 5: RIOK interacts with RARRES1 and TNFα induces apoptosis through RARRES1 and RIOK1**. (A) Podocytes were co-transfected with myc-DDK-tagged RIOK1 (RIOK1-myc-DDK) with either control EGFP vector, wildtype RARRES1-V5, or cleavage mutant FFAF-V5. Lysates were immunoprecipitated with V5 antibody to pull down the RARRES1-interacting proteins and probed with FLAG and RIOK-1 antibodies. Input lysates were probed with FLAG, RIOK1, V5, and GAPDH antibodies. (B) Human podocytes were transfected with overexpression plasmids of RARRES1-V5 and/or RIOK1-myc-DDK. Western blot analysis was performed 24 hours post transfection for phospho-p53 (ser46), cleaved Caspase-3, and RARRES1. (C) Podocytes stably transduced with lentiviral vector expressing scrambled control shRNA or *RARRES1* shRNA were treated with TNF-α (10 ng/ml for 24 hours). Lysates were probed for p-p53 (Ser46), RARRES1, and cleaved Caspase-3. The representative blots of three independent experiments are shown.

**Figure 6**

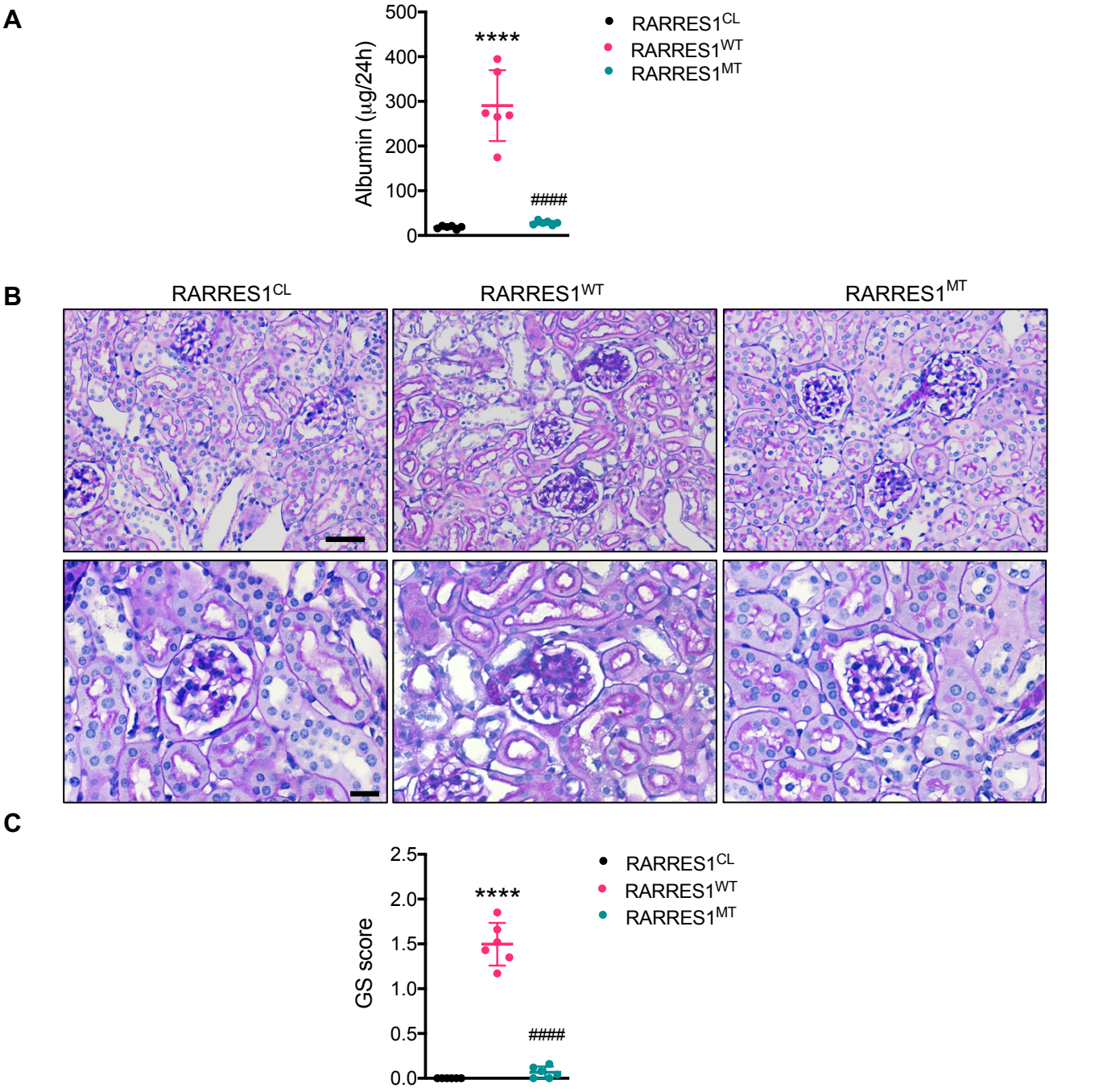


**Figure 6: Podocyte overexpression of RARRES$^{WT}$ induces glomerular injury.** (A) 24-hour albumin excretion. (B) Representative images of PAS-stained kidneys. Scale bars, 50µm (upper panel), 20µm (lower panel). (C) Average glomerulosclerosis (GS) score per glomerular cross section per mouse (n=6 mice per group, 25 glomeruli evaluated for each mouse, Data represents mean±SD).****P<0.0001 vs. RARRES1$^{CL}$; ####P<0.0001 vs. RARRES1$^{WT}$ by 1-way ANOVA with Tukey's multiple comparison test.

**Figure 7**

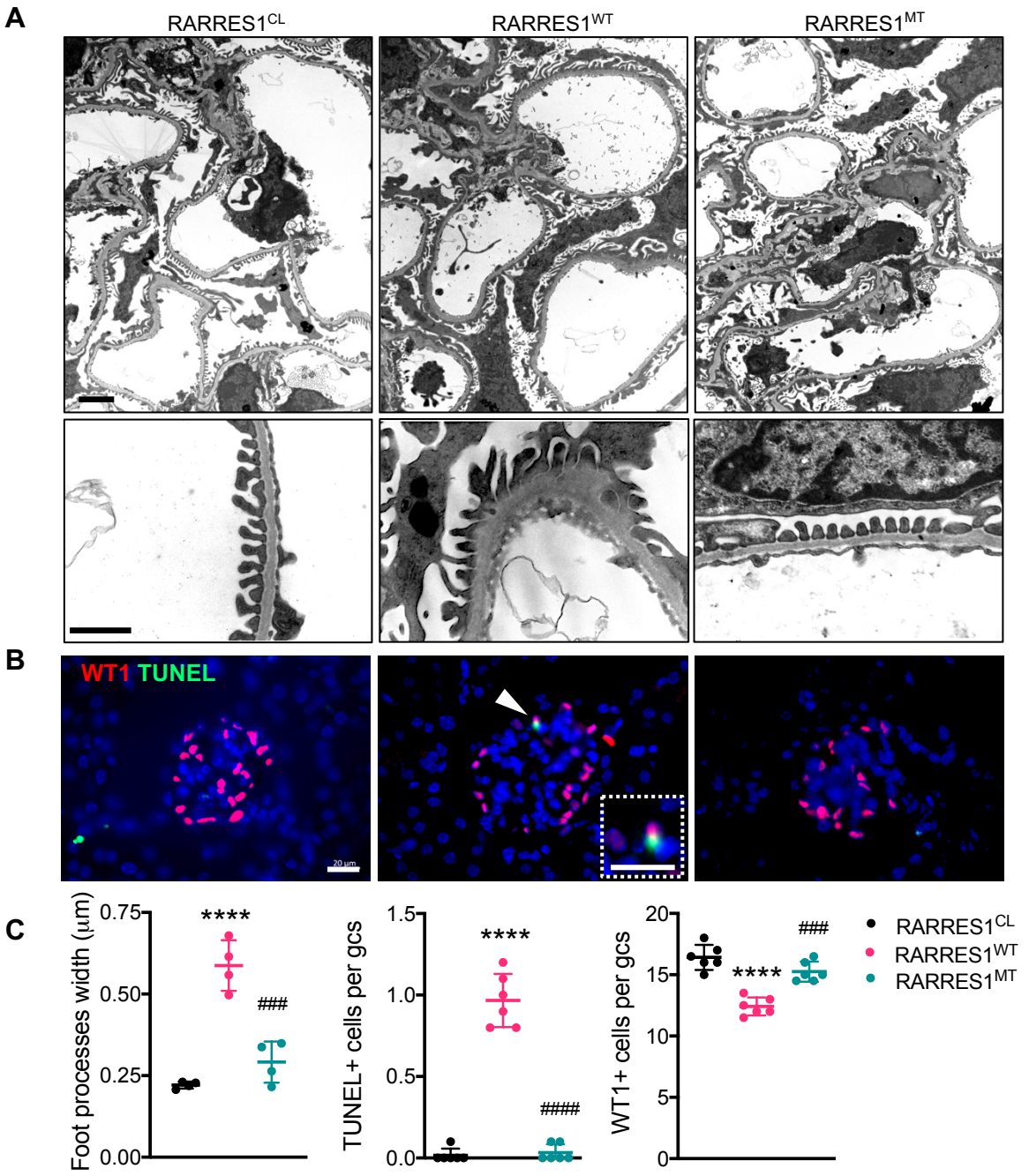


**Figure 7: Podocyte overexpression of RARRES$^{WT}$ induces podocyte injury and loss.** (A) Representative transmission EM images for low and high magnifications. Scale bars, 1µm. (B) Representative images of WT1 immunostaining (red) and TUNEL staining (green). Scale bar, 20µm. Arrowhead shows the WT1+ and TUNEL+ cell in RARRES$^{WT}$ kidney and magnified view is shown in the dotted inset. (C) Quantification of average foot process (n=4 mice per group evaluated) from TEM images (n=4 mice per group) and average TUNEL+ and WT1+ cells per glomerular cross section (gcs) per mouse (n=6 mice per group, 10 glomeruli evaluated for each mouse. All data represent mean±SD. ****P<0.0001 vs. RARRES1$^{CL}$; ###P<0.001 and ####P<0.0001 vs. RARRES1$^{WT}$ by 1-way ANOVA with Tukey's multiple comparison test.

**Figure 8**

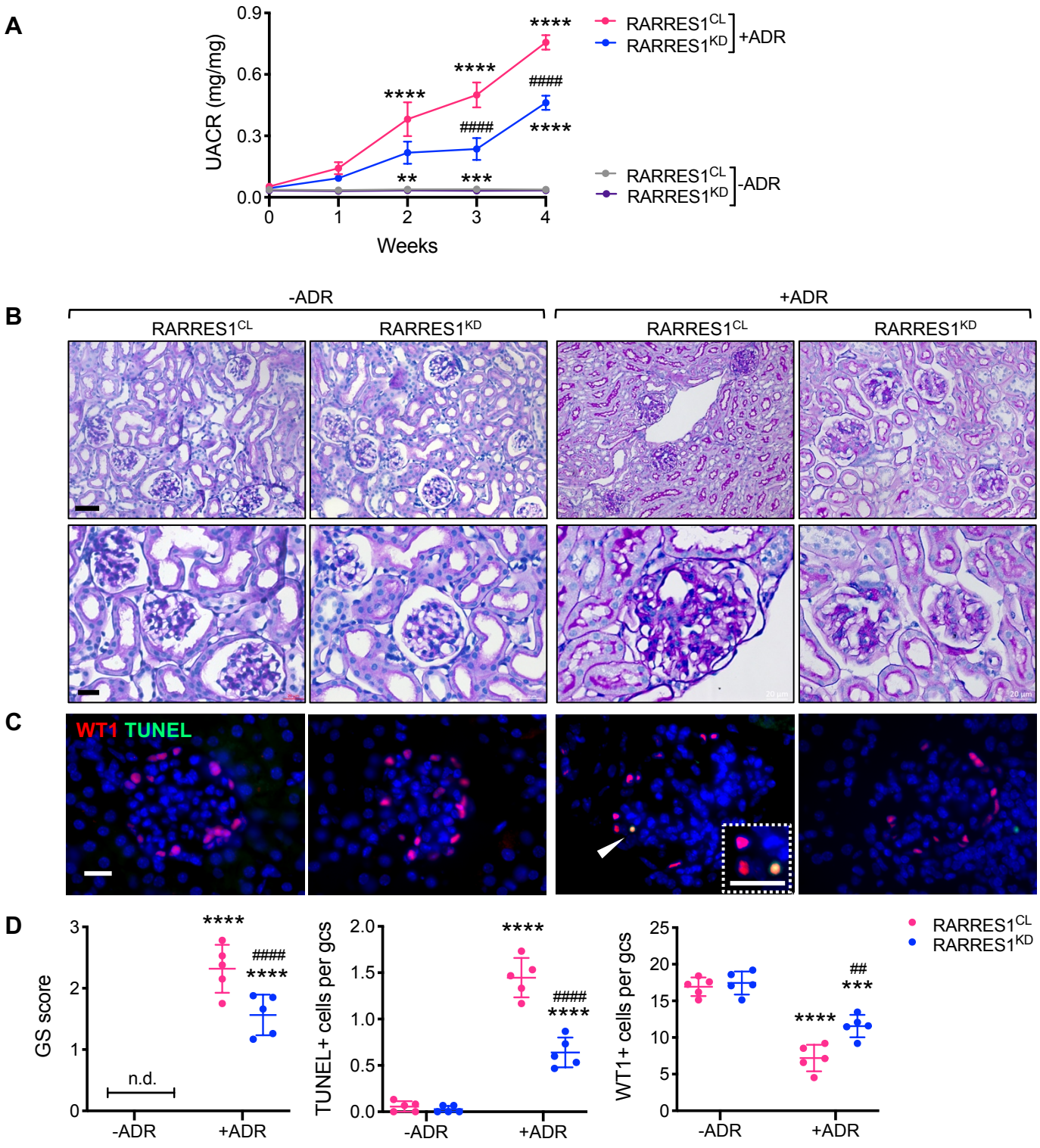


**Figure 8: Podocyte *Rarres1* knockdown attenuates albuminuria and glomerular injury in Adriamycin (ADR)-induced nephropathy in mice.** *Nphs1*-rtTA;TRE-*Rarres1*$^{KD}$ mice were given either control chow (RARRES1$^{CL}$) or Dox-supplemented chow (RARRES1$^{KD}$) for two weeks prior to ADR (+ADR) or vehicle (-ADR) injection. All mice were sacrificed after 4 weeks post injection. (A) UACR after ADR or vehicle injection, where week 0 indicates the baseline prior to injection. Data represent mean±SEM, n=5 mice per group. **P<0.01, ***P<0.001, and ****P<0.0001 vs. respective -ADR control; ####P<0.0001 vs. RARRES1$^{CL}$+ADR by 2-way ANOVA with Tukey's multiple comparison test. (B) Representative images of PAS-stained kidneys. Original magnification, x200 (upper panels, x400 (lower panels), Scale bar, 20μm. (C) Representative images of WT1 (red) and TUNEL (green) co-immunostaining. Scale bar, 20μm. A magnified view of WT1+ and TUNEL+ cell is shown in the inset. (D) Average glomerulosclerosis (GS) score per glomerular cross section per mouse (n=5 mice per group, 25 glomeruli evaluated for each mouse) and TUNEL+ and WT1+ cells per glomerular cross section (gcs) per mouse (n=5 mice per group, 15 glomeruli evaluated for each mouse). Data represent mean±SD, ***P<0.001 and ****P<0.0001 vs. -ADR control; ##P<0.01 and ####P<0.0001 vs. RARRES1$^{CL}$+ADR by 1-way ANOVA with Tukey's multiple comparison test.

**Figure 9**

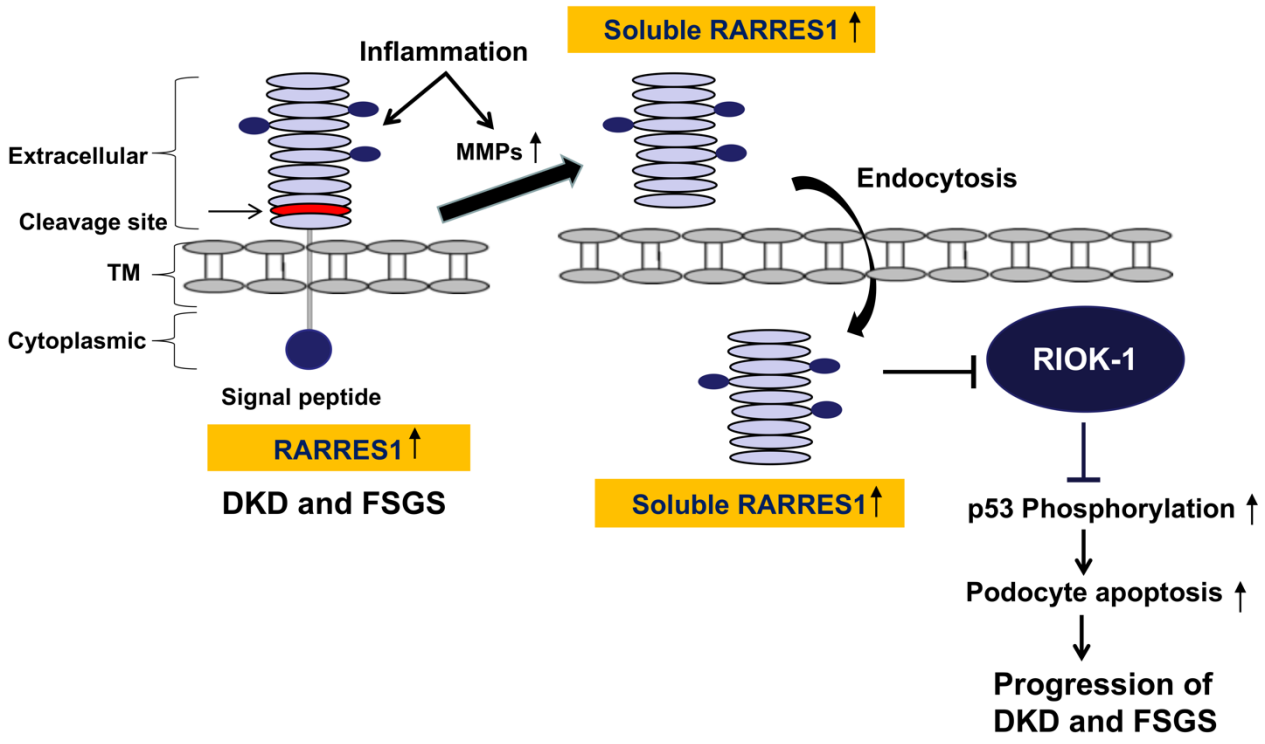


**Figure 9: Summary of the mechanism by which RARRES1 regulates podocyte apoptosis.** TNFα induces expression of RARRES1, which is cleaved into soluble RARRES1, potentially mediated by inflammation-stimulated MMP. The soluble RARRES1 is then endocytosed and interacts with intracellular RIOK1. The interaction between RIOK1 and RARRES1 leads to the inactivation of RIOK1, thereby activating p53 and apoptosis pathway. Podocyte loss is a key event for progression of DKD and FSGS.